

Supporting Information

Sub- 1 μm Free-standing Symmetric Membrane for Osmotic Separations

Wei Cheng^{2,3}, Jun Ma³, Xuan Zhang^{1,4*}, and Menachem Elimelech^{4*}

- 1) *Key Laboratory of New Membrane Materials, Ministry of Industry and Information Technology, School of Environmental and Biological Engineering, Nanjing University of Science & Technology, Nanjing 210094, China*
- 2) *Key Laboratory of Drinking Water Science and Technology, Research Center for Eco-Environmental Sciences, Chinese Academy of Sciences, Beijing 100085, China*
- 3) *State Key Laboratory of Urban Water Resource and Environment, School of Environment, Harbin Institute of Technology, Harbin 150090, China*
- 4) *Department of Chemical and Environmental Engineering, Yale University, New Haven, Connecticut 06520-8286, USA*

***Corresponding Authors:**

Xuan Zhang: xuanzhang@njust.edu.cn;

Menachem Elimelech: menachem.elimelech@yale.edu.

SUPPORTING DISCUSSION

Synthesis of Polybenzimidazole (PBI)

PBI was synthesized through the polycondensation of 3,3'-diaminobenzidine and 4,4'-oxybis (benzoic acid). A typical procedure involved the following steps. A 150 mL three-necked flask equipped with a magnetic stirrer, condenser, and nitrogen inlet/outlet was charged with 3,3'-diaminobenzidine (2.0 g, 9.334 mmol) and 20.0 g of polyphosphoric acid (PPA). After complete dissolution at 50 °C, 4,4'-oxybis (benzoic acid) (2.410 g, 9.334 mmol) and an additional portion of PPA (15.0 g) were added to the flask under N₂ atmosphere. The solution was successively heated at 150 °C for 1 hour, 180 °C for 1 hour, and 200 °C for 18 hours. The highly viscous solution was directly poured into a 2 wt% NaHCO₃ aqueous solution under vigorous stirring. The isolated fiber-like polymers were thoroughly washed with DI water, filtered, and dried under vacuum at 120 °C overnight (yield: 95%).

Synthesis of Sulfonated Polybenzimidazole (SPBI)

A typical synthesis procedure followed these steps. A 50 mL flask equipped with a magnetic stirrer was charged with PBI fibers (2.0 g) and 40.0 mL of concentrated sulfuric acid. After complete dissolution at room temperature, the solution was heated at certain temperatures for 24 hours. After cooling down, the viscous solution was carefully poured into a 2 wt% NaHCO₃ aqueous solution under vigorous stirring. The isolated fiber-like polymers were thoroughly washed with DI water until neutral, filtered, and dried under vacuum at 120 °C overnight. The polymers reacted at 60 and 70 °C were denoted as SPBI-60 and SPBI-70, respectively.

Preparation of PBI and SPBI Thin-film Membranes

All membranes were prepared by a solution casting method. In brief, a known amounts of the PBI or SPBI polymers were dissolved in NMP to form a homogeneous solution (1%, w/v), filtered through a 0.45 µm PTFE filter, and stored at room temperature overnight for degassing. Then, a certain volume of the solution was poured onto a clean and smooth Si wafer (University Wafer), extended to circular type with an approximate diameter of 3 cm, and placed on the top of a horizontally-adjusted hot plate, allowing for a complete evaporation of the solvent at 90 °C for 5-10 minutes. After immersing the Si wafer in DI water, transparent thin films were easily detached and floated on water. These membranes were then stored in DI water before property

characterization and performance evaluation. The Si wafer was cleaned with HCl and ethanol before and after use.

Characterization

^1H nuclear magnetic resonance (NMR) spectroscopy (Bruker Avance spectrometer) was performed in $\text{DMSO-}d_6$ to demonstrate the chemical structure of PBI and SPBI. The morphologies and thicknesses of the membranes were observed by surface and cross-sectional SEM (SU-70, Hitachi, Japan) images, respectively, followed by spin-coating a 10-nm-thick iridium film. SEM images of the SPBI-60 membrane with various thicknesses were also employed to demonstrate the surface segregation phenomenon of sulfonate groups. Specifically, the SPBI-60 membranes were immersed in 0.5 M CsCl solution overnight for ion exchange from H^+ ($-\text{SO}_3\text{H}$) to Cs^+ ($-\text{SO}_3\text{Cs}$) and dried under vacuum at room temperature. The water contact angle of the membranes was measured by OneAttension tensiometer (Biolin Scientific). Tensile-strain test (Series 5542, Instron, MA) was used to determine the mechanical properties of the membranes, with dimensions of 40 mm in length and 5 mm in width, at an elongation rate of 0.5 mm min^{-1} at 25°C and ambient atmosphere. Membrane surface charge was characterized by streaming potential using an electrokinetic analyzer with a set of AgCl electrodes (SurPASS^{III}, AntonPaar, Austria). For the streaming potential measurements, an electrolyte solution of 0.01 M KCl was used to provide the background ionic strength and was automatically titrated with 0.05 M HCl and 0.05 M NaOH to investigate the effect of pH on the zeta potential. Atomic force microscopy (AFM) was used to measure the interfacial forces between a functionalized particle probe and the membrane surface. The probe (PT.PS.COOH, Novascan Technologies, Inc) was composed of a COOH-functionalized polystyrene particle ($4.5 \text{ }\mu\text{m}$) attached to a silicon nitride cantilever (0.5 N/m). Force measurements were conducted in a fluid cell with a closed input/output loop.¹ Solution conditions tested were similar to those used in the bench-scale osmotic desalination experiments. Before injection of each solution, the cell was rinsed with 5 mL of deionized water and another 5 mL of the test solution (10 mM Na_2SO_4). After injection, the membrane was equilibrated with the test solution for at least 30 min before force measurement. Because of possible local membrane surface heterogeneities, force measurements were performed at five different locations on a $1 \text{ }\mu\text{m} \times 1 \text{ }\mu\text{m}$ area. At least five measurements were taken at each location.

Membrane Desalination Performance Tests

The water flux (J_w) and reverse solute flux (J_s) of the SPBI membranes were measured by a diffusion cell (PermeGear, Inc) under osmotic pressure driving force as described by Lu et al.² Briefly, the diffusion cell consists of two glass chambers for containing feed solution and draw solution, respectively, with a volume of 7 mL for each chamber. DI water was used as the feed solution and Na₂SO₄ solution at various concentrations ranging from 0.5 to 1.5 M was used as the draw solution. The effective area of membrane is 0.246 cm². The feed and draw solutions were stirred vigorously and the solution temperature was maintained at 25 °C during the measurements. A narrow graduated cylinder was equipped on the chamber of the draw solution to determine J_w , while the increase of salt concentration in the feed solution was determined by electric conductivity meter to obtain J_s :

$$J_w = \frac{\Delta V}{A_s \Delta t} \quad (S1)$$

$$J_s = \frac{C_f(V_0 - \Delta V)}{A_s \Delta t} \quad (S2)$$

where ΔV is the increase in volume of draw solution in the graduated cylinder, A_s is the membrane area, Δt is time, C_f is the solute concentration in the feed solution at the end of the test, and V_0 is the initial volume of the feed solution.

Evaluation of Membrane Transport Parameters (A , B , S)

Water permeability coefficient (A), salt permeability coefficient (B), and solute rejection (R) of the SPBI membranes were determined in a lab-scale crossflow RO system as described elsewhere.³ The crossflow velocity and temperature during the experiments were 39 cm s⁻¹ and 25 °C, respectively. The membrane was equilibrated with DI water at a pressure of 18 bar (260 psi) for 1 h to obtain a stable flux. After equilibration, the pressure (ΔP) was set to 15 bar (220 psi) to obtain the A value with DI water and the R value with Na₂SO₄ (7 mmol L⁻¹):

$$A = J_w^{RO} / \Delta P \quad (S3)$$

$$R = \left(1 - \frac{C_p}{C_f}\right) \times 100\% \quad (S4)$$

where J_w^{RO} is the DI water flux of the membrane in RO, C_f is the concentration of feed solution (7 mmol L⁻¹ Na₂SO₄), and C_p is the concentration of permeate. C_f and C_p were obtained by measuring the electric conductivity of the respective solutions.

The salt permeability coefficient, B , was determined from⁴⁻⁷

$$B = J_w^{RO} \frac{1-R}{R} \exp \left(-\frac{J_w^{RO}}{k} \right) \quad (S5)$$

where k is the mass transfer coefficient obtained from

$$k = \frac{ShD}{d_h} \quad (S6)$$

where D is the diffusion coefficient of Na_2SO_4 , d_h is the hydrodynamic diameter of the channel, and Sh is the Sherwood number obtained from

$$Sh = 1.86(ReSc \frac{d_h}{L})^{0.33} \quad (S7)$$

where L is the length of the flow channel, and Re and Sc are the Reynolds number and the Schmidt number, respectively:

$$Re = \frac{u d_h \rho}{\mu} \quad (S8)$$

$$Sc = \frac{\mu}{\rho D} \quad (S9)$$

where ρ is the water density, μ is the dynamic viscosity of the solution, and u is the crossflow velocity.

The membrane resistance to solute diffusion, K , is thus obtained using^{8, 9}

$$K = \frac{1}{J_w^{FO}} \ln \frac{B + A\pi_d}{B + J_w^{FO} + A\pi_f} \quad (S10)$$

where π_d and π_f are the osmotic pressures of the draw solution (1.5 M Na_2SO_4) and feed solution (0 bar for DI water), respectively. The structural parameter (S) of the membrane was calculated from

$$S = KD \quad (S11)$$

Membrane Water Uptake (WU) and Dimensional Change (DC)

WU and DC (in-plane direction, ΔL) of all membranes were measured by the following methods. The membrane samples were cut into rectangular pieces (3 cm \times 1 cm), dried at 120 °C for 2 h under vacuum, and taken out to measure the weight and dimension to serve as the reference. Then, the films were immersed in DI water at 25 °C for at least 2 h, taken out, and quickly weighed on the counter balance. WU and ΔL were then calculated from

$$\text{WU} = \frac{w_1 - w_0}{w_0} \times 100\% \quad (S12)$$

$$\Delta L = \frac{L_1 - L_0}{L_0} \times 100\% \quad (\text{S13})$$

where, W_1 and W_0 refer to the weights of the wet and dry membranes, and L_1 and L_0 refer to the lengths of the wet and dry membranes, respectively.

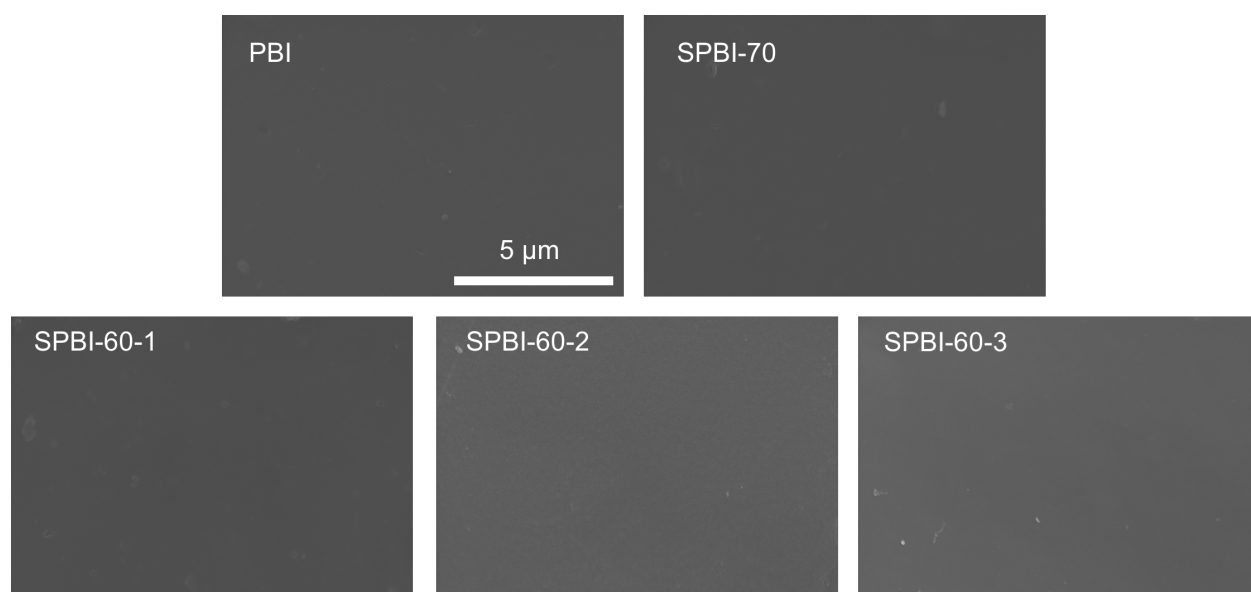


Figure S1. SEM images of the bottom surfaces of the PBI, SPBI-70, and SPBI-60 membranes.

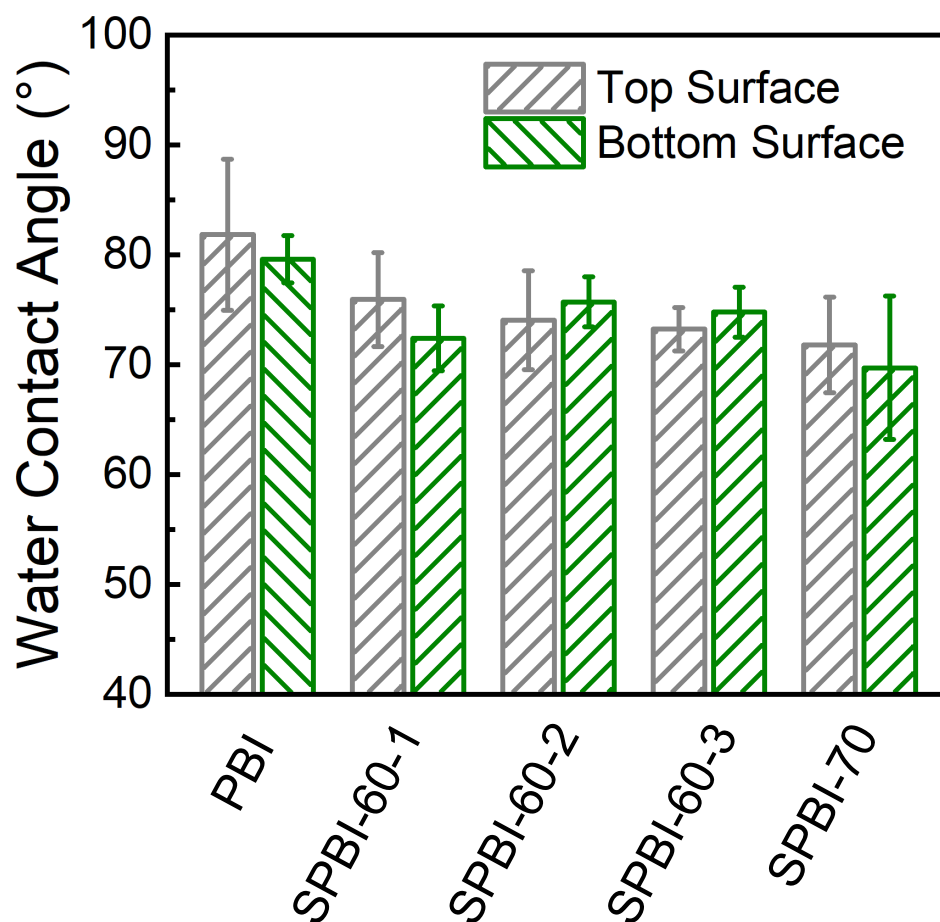


Figure S2. Water contact angle of the top surface (grey) and bottom surface (green) of the PBI and SPBI membranes. DI water drop (1 μ L) was placed on the surface of membranes and seven measurements at random locations were applied for each sample. Error bars represent standard deviation.

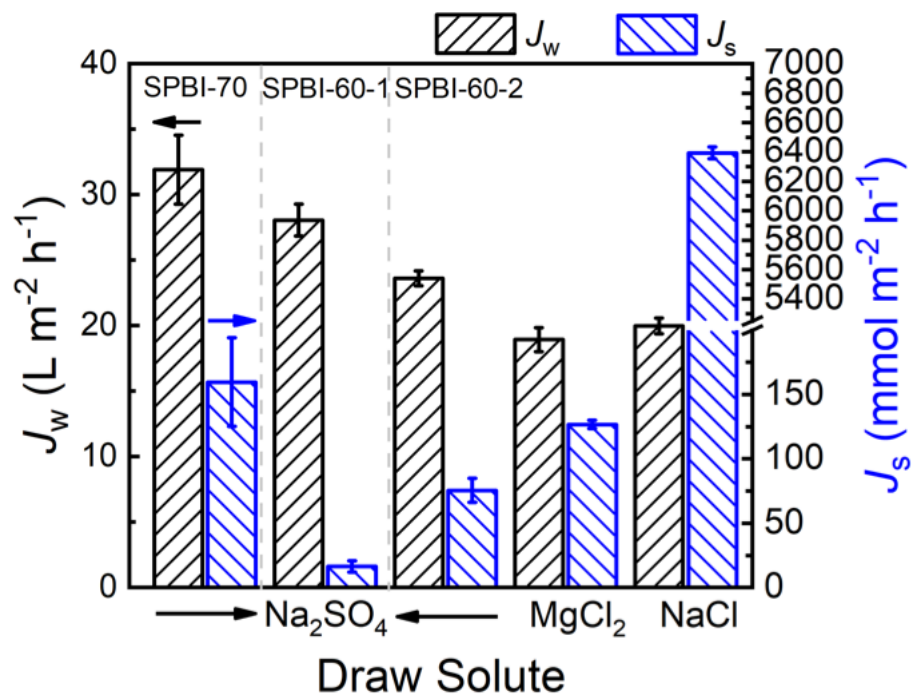


Figure S3. Water flux (left axis) and reverse salt flux (right axis) for the SPBI-70, SPBI-60-1, and SPBI-60-2 membranes with different types of draw solutes. 1.5 M Na_2SO_4 , 1.5 M MgCl_2 , and 2 M NaCl were chosen as the draw solutions, and DI water was used as the feed solution. It should be noted that the PBI membrane did not show water or salt under the tested conditions.

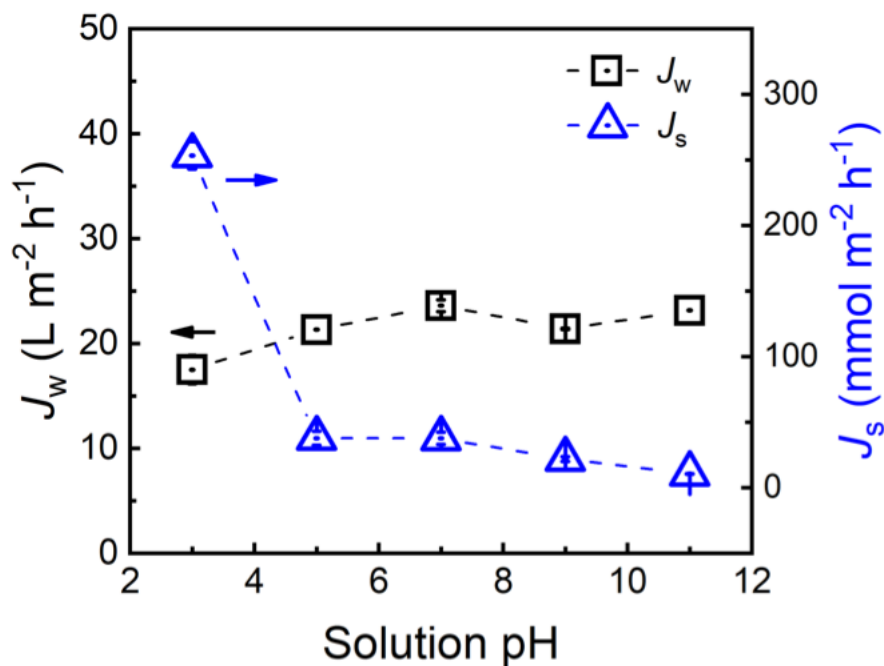


Figure S4. Water flux (J_w) and reverse salt flux (J_s) of the SPBI-60-2 membrane as a function of solution pH. The pH of feed solution (DI water) and draw solution (1.5 M Na_2SO_4) were adjusted by the addition of diluted sulfuric acid or sodium hydroxide solution. Ion chromatography (ICS-1000, Dionex, Sunnyvale, CA, USA) was used to measure the concentration of salt in the feed solution. Due to the existence of sulfuric acid and sodium hydroxide in the acidic and alkaline conditions, respectively, the concentration of Na^+ was measured to determine J_s in the acidic conditions, whereas SO_4^{2-} was measured in the basic conditions.

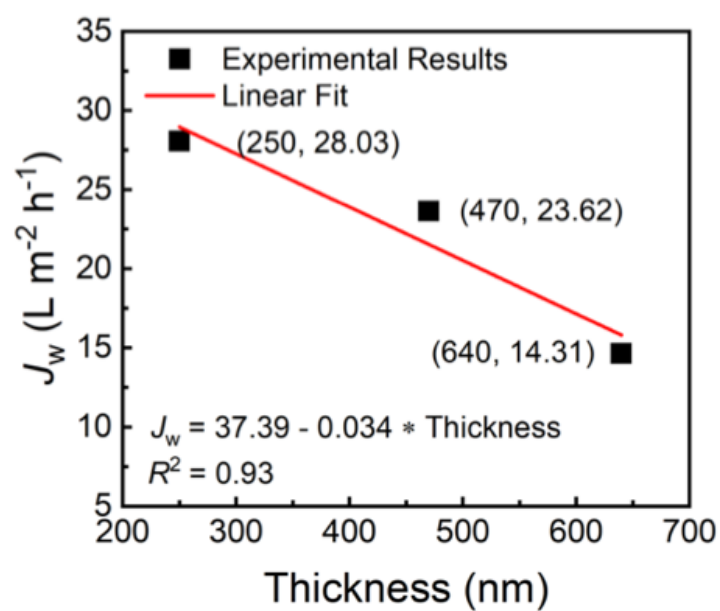


Figure S5. Water flux of the SPBI-60 membranes as a function of membrane thickness.

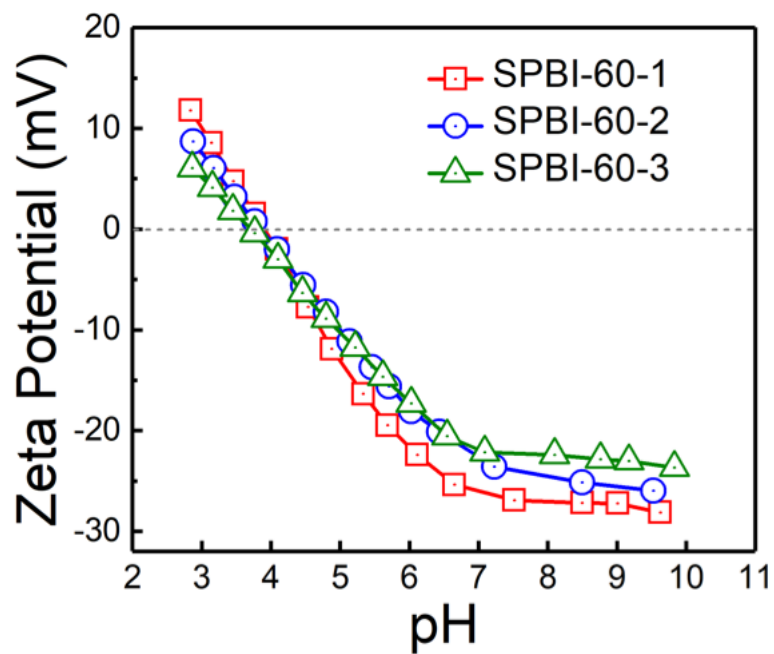


Figure S6. Zeta potential of the bottom surfaces of the SPBI-60 membranes with various thicknesses. An electrolyte solution of 0.01 M KCl was used as background solution, and 0.05 M HCl and 0.05 M NaOH solutions were automatically titrated to adjust the solution pH from 3 to 10.

Table S1 Thickness, chemical composition, and swelling properties of the SPBI membranes.

Entry	Nomenclature	Thickness (nm)	DS ^{a)} (%)	IEC ^{b)}	WU ^{c)} (%)	DC ^{d)} (%)
1	SPBI-60-1	250	0.163	0.66	4.0 ± 0.3	2.0 ± 0.5
	SPBI-60-2	470	0.163	0.66	3.7 ± 0.5	2.0 ± 0.5
	SPBI-60-3	640	0.163	0.66	3.6 ± 0.1	1.8 ± 0.5
2	SPBI-70	220	0.384	1.25	9.8 ± 0.6	8.4 ± 0.7

a) Degree of sulfonation of SPBI-60 and SPBI-70. DS can be calculated from the integration ratio of H(4') to all other aromatic protons in Figure 1B, according to the Equations S14 and S15 below; in these equations, x represents the sulfonated moiety and y represents the non-sulfonated moiety. b) Ion exchange capacity (IEC, meq g⁻¹, calculated from the x/y results, according to Equation S16 below. c) Water uptake by the membranes, measured in DI water at 25 °C according to Equation S12. d) Dimensional change of the membranes, measured in DI water at 25 °C according to Equation S13.

$$\frac{I(4')}{I(Ar-H)} = \frac{2x}{10x+14y} \quad (S14)$$

$$DS = x/y \quad (S15)$$

where I(4') and I(Ar-H) refer to the integration of H(4') and all other aromatic protons in Figure 1B.

$$IEC = \frac{1000 \times 2x}{560.55 + 400.44y} \quad (S16)$$

where 560.55 and 400.44 refer to the molecular weight (Da) of the sulfonated and non-sulfonated moiety in a repeating unit, respectively.

Table S2 Mechanical properties of PODH, PTAODH-1.0, PBI, and SPBIs membranes

Membrane	Elongation (%)	Young's Modulus (GPa)	Maximum Stress (MPa)
PODH ^{a)}	43.5	0.82	64.4
PTAODH-1.0 ^{a)}	6.7	1.31	71.2
PBI	8.51 ± 0.61	9.77 ± 0.24	72.85 ± 0.62
SPBI-60-1	17.80 ± 0.04	6.70 ± 0.65	62.87 ± 0.01
SPBI-70	12.99 ± 1.62	4.81 ± 0.19	49.55 ± 2.52

a) Li et al., ref (3).

References

1. Li, Q.; Elimelech, M., Organic Fouling and Chemical Cleaning of Nanofiltration Membranes: Measurements and Mechanisms. *Environ. Sci. Technol.* **2004**, *38*, 4683-4693.
2. Lu, X.; Feng, X.; Zhang, X.; Chukwu, M. N.; Osuji, C. O.; Elimelech, M., Fabrication of a desalination membrane with enhanced microbial resistance through vertical alignment of graphene oxide. *Environ. Sci. Technol. Lett.* **2018**, *5*, 614-620.
3. Li, M.; Karanikola, V.; Zhang, X.; Wang, L.; Elimelech, M., A self-standing, support-free membrane for forward osmosis with no internal concentration polarization. *Environ. Sci. Technol. Lett.* **2018**, *5*, 266-271.
4. Lu, X.; Arias Chavez, L. H.; Romero-Vargas Castrillón, S.; Ma, J.; Elimelech, M., Influence of Active Layer and Support Layer Surface Structures on Organic Fouling Propensity of Thin-Film Composite Forward Osmosis Membranes. *Environ. Sci. Technol.* **2015**, *49*, 1436-1444.
5. Yip, N. Y.; Tiraferri, A.; Phillip, W. A.; Schiffman, J. D.; Elimelech, M., High performance thin-film composite forward osmosis membrane. *Environ. Sci. Technol.* **2010**, *44*, 3812-3818.
6. Baker, R. W., *Membrane Technology and Applications*. 2nd ed ed.; Wiley: New York: **2004**; p 552.
7. Mulder, M., *Basic Principles of Membrane Technology*. 2nd ed ed.; Kluwer Academic Publisher: The Netherlands: **1996**; p 421.
8. Cath, T.; Childress, A.; Elimelech, M., Forward osmosis: Principles, applications, and recent developments. *J. Membr. Sci.* **2006**, *281*, 70-87.
9. Loeb, S.; Titelman, L.; Korngold, E.; Freiman, J., Effect of porous support fabric on osmosis through a Loeb-Sourirajan type asymmetric membrane. *J. Membr. Sci.* **1997**, *129*, 243-249.